Thermal Decomposition of the Perfluorinated Peroxides $CF_3OC(O)OOC(O)F$ and $CF_3OC(O)OOCF_3$

Maximiliano A. Burgos Paci and Gustavo A. Argüello*

INFIQC, Departamento de Físico Química, Facultad de Ciencias Químicas, Universidad Nacional de Córdoba, Ciudad Universitaria, 5000 Córdoba, Argentina

Plácido García and Helge Willner

Fachbereich C, Anorganische Chemie, Bergische Universität Wuppertal, D-42119 Wuppertal, Germany

Received: May 31, 2005; In Final Form: July 1, 2005

Gas phase thermal decomposition of $CF_3OC(O)OOC(O)F$ and $CF_3OC(O)OOCF_3$ was studied at temperatures between 64 and 98 °C ($CF_3OC(O)OOC(O)F$) and 130−165 °C ($CF_3OC(O)OOCF_3$) using FTIR spectroscopy to follow the course of the reaction. For both substances, the decompositions were studied with N_2 and CO as bath gases. The rate constants for the decomposition of $CF_3OC(O)OOC(O)F$ in nitrogen and carbon monoxide fit the Arrhenius equations $k_{N_2} = (3.1 \pm 0.1) \times 10^{15} \exp[-(29.0 \pm 0.5 \text{ kcal mol}^{-1}/RT)]$ and $k_{CO} = (5.8 \pm 1.3) \times 10^{15} \exp[-(29.4 \pm 0.5 \text{ kcal mol}^{-1}/RT)]$, and that for $CF_3OC(O)OOCF_3$ fits the equation $k = (9.0 \pm 0.9) \times 10^{13} \exp[-(34.0 \pm 0.7 \text{ kcal mol}^{-1}/RT)]$ (all in units of inverted seconds). Rupture of the O−O bond was shown to be the rate-determining step for both peroxides, and bond energies of 29 ± 1 and 34.0 ± 0.7 kcal mol^{-1} were obtained for $CF_3OC(O)OOC(O)F$ and $CF_3OC(O)OOCF_3$. The heat of formation of the $CF_3OCO_2^{\bullet}$ radical, which is a common product formed in both decompositions, was calculated by ab initio methods as −229 ± 4 kcal mol^{-1}. With this value, the heat of formation of the title species and of $CF_3OC(O)OOC(O)OCF_3$ could in turn be obtained as $\Delta_f H^\circ_{298}(CF_3OC(O)OOC(O)F) = -286 \pm 6$ kcal mol^{-1}, $\Delta_f H^\circ_{298}(CF_3OC(O)OOCF_3) = -341 \pm 6$ kcal mol^{-1}, and $\Delta_f H^\circ_{298}(CF_3OC(O)OOC(O)OCF_3) = -430 \pm 6$ kcal mol^{-1}.

Introduction

Since the replacement of chlorofluorocarbons (CFCs) by compounds commonly designated as hydrofluorocarbons (HFCs), there have been exhaustive studies of the mechanism, intermediates, and final products of the HFC degradation reactions.[1] Along with these, in the past decade, much work has been devoted to the study of the properties and reactions of many compounds and radicals containing only F, C, and O atoms, that can be formed in the laboratory as a result of the degradation of HFCs in the presence of oxygen and high concentrations of CO. The study of these reactions afforded many new compounds to be synthesized and used as precursors of atmospherically relevant radicals which were thus isolated.[2−4] Several such compounds have been known for many years (e.g., $CF_3OC(O)OOCF_3$[5] and $FC(O)OOC(O)F$[6]), and many others have been discovered and characterized recently (e.g., $CF_3OC(O)OOC(O)OCF_3$,[7] $CF_3OC(O)OOOC(O)OCF_3$,[8] $CF_3OC(O)OOC(O)F$,[9] and $FC(O)OOOC(O)F$[10]). $CF_3OC(O)OOCF_3$ has been known since 1973,[5] and it is nowadays easily obtained as a byproduct of the $CF_3OC(O)OOC(O)OCF_3$ synthesis.[7] It was characterized by the team who first synthesized it, but its structure is still unknown. $CF_3OC(O)OOC(O)F$, in turn, was first mentioned[11] a couple of years ago, and it has been isolated only recently.[9]

Kinetic data on thermal decomposition are needed in order to have reliable estimates of bond energies and to help in the elucidation of mechanisms and in the calculation of thermodynamic properties. Nevertheless, for fluorocarbonoxygenated peroxides and trioxides, this kind of studies has been reported for just a few compounds such as CF_3OOCF_3,[12] CF_3OOOCF_3,[13] and $CF_3OC(O)OOC(O)OCF_3$.[14] In the present work, thermal decomposition rate constants have therefore been measured as a function of temperature and in the first-order region for $CF_3OC(O)OOC(O)F$ and $CF_3OC(O)OOCF_3$, thus providing new data to add to the available databases.

One common primary dissociation product of these two peroxides should be the radical $CF_3OCO_2^{\bullet}$, about which very little is known.[15] We contribute a theoretical study about this important and elusive radical with the goal of deriving some properties such as its structural parameters, vibrational spectrum, and heat of formation.

Results

$CF_3OC(O)OOC(O)F$. The thermal decomposition of $CF_3OC(O)OOC(O)F$ was evaluated at 14 different temperatures between 64 and 98 °C using N_2 or CO as bath gases, at total pressures of 1000 mbar in N_2 and 500 mbar in CO. No discernible effect of either total pressure or nature of the diluent gas was observed on the decomposition rate. The disappearance of the reagent was followed using its absorption bands at 1874 and 969 cm^{-1} after subtraction of the interfering products. The data were analyzed according to first-order kinetics:

$$-\frac{d[CF_3OC(O)OOC(O)F]}{dt} = k_{exptl}[CF_3OC(O)OOC(O)F] \quad (1)$$

Figure 1 shows plotting of the logarithms of absorbance versus time for reactant loss in N_2 as diluent (plots for CO as

* Corresponding author. E-mail: gaac@fisquim.fcq.unc.edu.ar.

10.1021/jp0528818 CCC: $30.25
Published on Web 08/04/2005

TABLE 1: First-Order Rate Constants from Decomposition of the Peroxides in N_2 or CO at Different Temperatures[a]

$CF_3OC(O)OOC(O)F$				$CF_3OC(O)OOCF_3$			
in N_2		in CO		in N_2		in CO	
T	k	T	k	T	k	T	k
64.0	$(6.11 \pm 0.12) \times 10^{-4}$	62.0	$(5.07 \pm 0.74) \times 10^{-4}$	130	$(3.80 \pm 0.25) \times 10^{-5}$	130	$(3.66 \pm 0.07) \times 10^{-5}$
71.0	$(1.66 \pm 0.02) \times 10^{-3}$	72.0	$(1.71 \pm 0.01) \times 10^{-3}$	140	$(1.26 \pm 0.05) \times 10^{-4}$	135	$(6.83 \pm 0.26) \times 10^{-5}$
78.0	$(4.06 \pm 0.43) \times 10^{-3}$	79.0	$(3.13 \pm 0.04) \times 10^{-3}$	150	$(3.02 \pm 0.06) \times 10^{-4}$	140	$(1.13 \pm 0.02) \times 10^{-4}$
83.0	$(6.43 \pm 0.07) \times 10^{-3}$	88.0	$(6.32 \pm 0.19) \times 10^{-3}$	160	$(7.22 \pm 0.13) \times 10^{-4}$	144	$(1.81 \pm 0.07) \times 10^{-4}$
88.0	$(9.73 \pm 0.07) \times 10^{-3}$	93.0	$(1.20 \pm 0.04) \times 10^{-2}$			149	$(4.32 \pm 0.33) \times 10^{-4}$
98.0	$(3.20 \pm 0.06) \times 10^{-2}$					155	$(4.82 \pm 0.12) \times 10^{-4}$
						159	$(7.19 \pm 0.15) \times 10^{-4}$
						160	$(5.81 \pm 0.28) \times 10^{-4}$
						165	$(1.21 \pm 0.02) \times 10^{-3}$

[a] Temperature in °C. First-order constants, k, in s^{-1}.

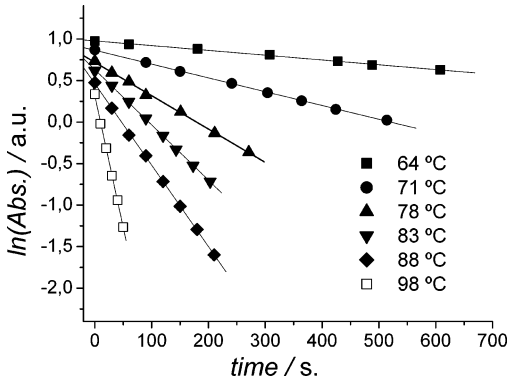

Figure 1. First-order kinetic curves at selected temperatures for the decomposition of $CF_3OC(O)OOC(O)F$ in N_2 as diluent.

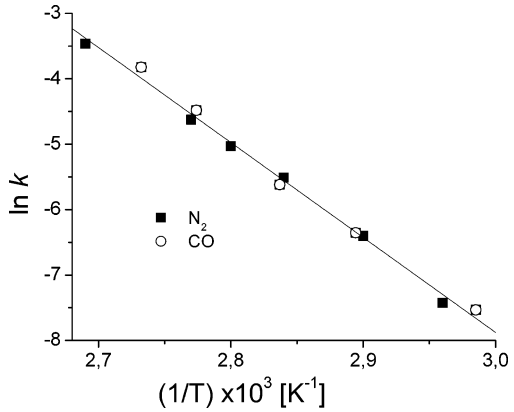

Figure 2. Arrhenius plot for the decomposition of $CF_3OC(O)OOC(O)F$ in N_2 and CO diluents.

diluent are of the same quality). Good straight lines were obtained in all cases. At each temperature studied, the first-order rate constant was calculated from the plot by a least-squares method. Average rate constants are given in Table 1 along with the values obtained for CO as diluent gas.

The rate constants are also graphically shown in Figure 2 in the form of an Arrhenius plot. The least-squares analysis of the data gave the expressions

$$k_{\text{exptl},N_2}[CF_3OC(O)OOC(O)F] = (3.1 \pm 0.9) \times 10^{15}\ s^{-1} \exp\left[-\frac{29.0 \pm 0.5\ \text{kcal mol}^{-1}}{RT}\right]$$

$$k_{\text{exptl,CO}}[CF_3OC(O)OOC(O)F] = (5.8 \pm 1.3) \times 10^{15}\ s^{-1} \exp\left[-\frac{(29.4 \pm 0.5)\ \text{kcal mol}^{-1}}{RT}\right] \quad (2)$$

where it can be seen that the first-order constants in N_2 and CO are the same within experimental error, and then, $k_{\text{exptl}} = (3.1 \pm 2.0) \times 10^{15}\ s^{-1} \exp[-(29.2 \pm 0.5\ \text{kcal·mol}^{-1}/RT)]$.

Figure 3 shows the IR spectra of the products when the reactions are carried out in N_2 (part A) and CO (part B). These spectra were obtained at the end of the reaction after suitable subtraction of the reagent. As seen in Figure 3, when N_2 is the bath gas, $CF_3OC(O)OOC(O)F$ decomposition results in the formation of CO_2 (2300 cm^{-1}), $CF_3OOC(O)F$ (1922, 1296, 1245, and 1172 cm^{-1}), and CF_2O (773 cm^{-1}), while an additional product, $CF_3OC(O)F$ (1258 and 1179 cm^{-1}), appears when CO is the bath gas. Some new bands are also observed which could not be unambiguously assigned (1848, 1818, and 1055 cm^{-1}).

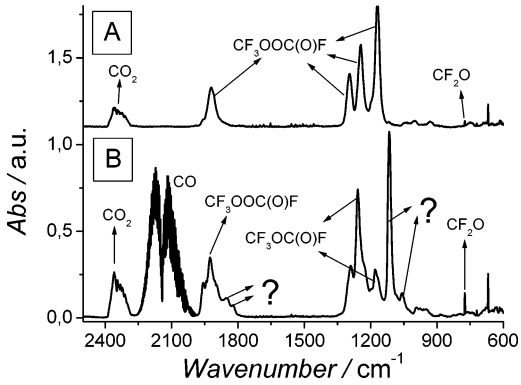

Figure 3. IR spectra of the products obtained in the decomposition of $CF_3OC(O)OOC(O)F$ in N_2 (A) and CO (B) diluents.

$CF_3OC(O)OOCF_3$. The kinetics of $CF_3OC(O)OOCF_3$ decomposition was studied between 130 and 165 °C at a total pressure of 1000 mbar using N_2 or CO as bath gases. The disappearance of the reagent was monitored via its absorption band at 1884 cm^{-1}. As in the case of $CF_3OC(O)OOC(O)F$, the data were analyzed in terms of first-order kinetics.

In Figure 4, first-order plots for the decompositions in N_2 are presented. In all cases, the experimental points and the linear fit are in very good agreement. Table 1 shows the first-order constants obtained from these plots.

To evaluate the Arrhenius parameters, all of the determined rate constants were used to construct an Arrhenius plot, irrespective of the bath gas used. Linear least-squares analysis of the data in Figure 5 gives

$$k_{\text{exptl}}[CF_3OC(O)OOCF_3] = (9.0 \pm 0.9) \times 10^{13}\ s^{-1} \exp\left[-\frac{34.0 \pm 0.7\ \text{kcal mol}^{-1}}{RT}\right] \quad (3)$$

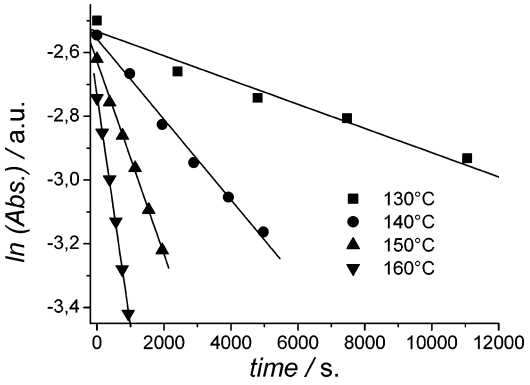

Figure 4. First-order kinetic curves at selected temperatures for the decomposition of $CF_3OC(O)OOCF_3$ in N_2 as diluent.

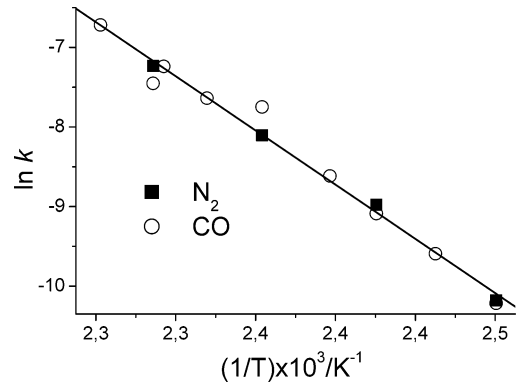

Figure 5. Arrhenius plot for the decomposition of $CF_3OC(O)OOF_3$.

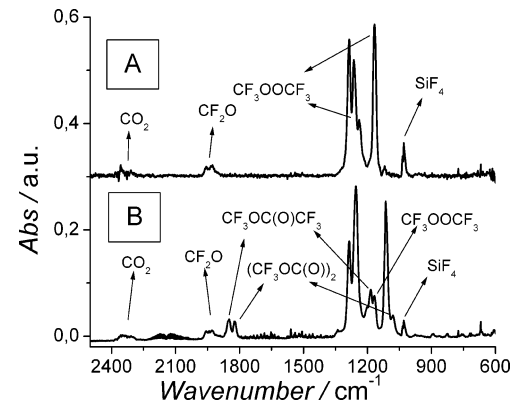

Figure 6. IR spectra of the products obtained from the decomposition of $CF_3OC(O)OOCF_3$ in N_2 (A) and CO (B) diluents.

Figure 6 shows the IR spectra of the products obtained using N_2 (part A) and CO (part B) as diluents. In the former case, the decomposition gives CF_3OOCF_3 (1285, 1262, and 1167 cm^{-1}), CF_2O, CO_2, and SiF_4 (1028 cm^{-1}), and in the latter case, besides the products obtained before, $(CF_3OC(O))_2$ (1820, 1114, and 1080 cm^{-1}) and $CF_3OC(O)CF_3$ (1850 and 1184 cm^{-1}) are formed.

Discussion

$CF_3OC(O)OOC(O)F$ decomposition was studied at total pressures of 1000 and 500 mbar of N_2 and CO, respectively. Since the rate constants were independent of total pressure, it is assumed that these data are in the high pressure region, as expected for such a complex molecule. Examples of similar species that achieve their first-order values at pressures of around 500 mbar are $(CF_3OC(O)O)_2$,[14] $(CH_3C(O)O)_2$,[16] CF_3OOOCF_3,[17] and $CH_3C(O)OONO_2$.[18]

TABLE 2: Pre-exponential Factors and Entropy of Activation for Selected Molecules

molecule	A factors	$\Delta S^{\#}$ (eu)	ref
$CF_3OC(O)OOC(O)F$	$10^{15.6}$	10.5	this work
$CF_3OC(O)OOCF_3$	$10^{13.9}$	2.0	this work
$CF_3OC(O)OOC(O)OCF_3$	$10^{14.5}$	5.5	14
$CF_3OC(O)OOOC(O)OCF_3$	$10^{12.9}$	1.0	8
$CH_3C(O)OOC(O)CH_3$	$10^{14.2}$	3.7	47
$C_2H_5C(O)OOC(O)C_2H_5$	$10^{14.4}$	4.5	48
$C_3H_7C(O)OOC(O)C_3H_7$	$10^{14.3}$	4.0	48

The measured Arrhenius parameter is entirely reasonable for a homogeneous gas phase decomposition of a large molecule into two smaller free radical fragments. The high A factor obtained ($10^{15.6}$ s^{-1}) reflects the increase in entropy associated with the formation of a loose transition state in which free rotation about the breaking bond can occur and two relatively large fragments are generated.

The thermal decomposition of $CF_3OC(O)OOCF_3$ has been investigated carrying out experiments to cover the range between 165 and 130 °C and for pressure ranges that ensure first-order behavior. The derived activation energy is 34.0 kcal/mol, and the extrapolated A factor is $10^{13.9}$, thus giving an activation entropy of 2.0 eu. The A factor is somewhat lower than the one for $CF_3OC(O)OOC(O)F$; nevertheless, we still believe the decomposition directly provides two smaller fragments in a simple bond fission. The difference in A factors could be rationalized in terms of the π stabilization afforded by the two fragments formed. In Table 2, the pre-exponential factors of closely related molecules are presented. It can be seen that the hydrogenated peroxides have almost the same A factor (ranging from $10^{14.2}$ to $10^{14.4}$) as the fluorinated peroxide $CF_3OC(O)$-$OOC(O)OCF_3$ (with an A factor of $10^{14.5}$). All of these peroxides form two equally bulky and delocalized carboxy radicals when decomposed. In the case of $CF_3OC(O)OOC(O)F$, two contributions to π stabilization are possible: one through the $FCO_2^{\bullet}$ radical[19] and the other through $CF_3OCO_2^{\bullet}$. Nevertheless, when only one of these delocalized radicals is formed, there seems to be a lowering in the A factor, as can be seen for both CF_3-$OC(O)OOCF_3$ and the trioxide $CF_3OC(O)OOOC(O)OCF_3$. Furthermore, the decomposition reaction for the trioxide has been proved to be a simple bond fission by performing low temperature matrix experiments[3] where the $CF_3OC(O)OO^{\bullet}$ radical could be trapped despite the low A factor measured.[8]

We present below the mechanism for the pyrolysis of each peroxide that would account for eqs 2 and 3 and for the products obtained. In agreement with the above arguments, the first step in the decomposition process should be the breaking of the peroxide bond, which is the weakest in the molecule.

$CF_3OC(O)OOC(O)F$. The O−O rupture in $CF_3OC(O)OOC$-$(O)F$ produces $CF_3OCO_2^{\bullet}$ and $FCO_2^{\bullet}$ radicals

$$CF_3OC(O)OOC(O)F \rightarrow CF_3OCO_2^{\bullet} + FCO_2^{\bullet} \qquad (4)$$

Both carboxy radicals are susceptible to decarboxylation; however, our IR results indicate that the more abundant products formed bear the FCO_2. Thus, the decarboxylation process should be faster for $CF_3OCO_2^{\bullet}$ than for $FCO_2^{\bullet}$. The half-life for $FCO_2^{\bullet}$ has been reported to be ≈3 s at room temperature,[20] while for $CF_3OCO_2^{\bullet}$ it was assumed to be $\approx 10^{-4}$ s. This value corresponds to the decarboxylation of the $CF_3CO_2^{\bullet}$ radical, since the rate constant for $CF_3OCO_2^{\bullet}$ decomposition has not been measured so far and it is a common practice to resort to similar species.[21] Though arbitrary, the value for the half-life, $t_{1/2}$, is entirely consistent with experiments carried out in our lab and

reported elsewhere,[15] in which only below room temperature can the radical stabilize. The next step in the mechanism is probably the decarboxylation of the $CF_3OCO_2^\bullet$ radicals to produce $CF_3O^\bullet$ and CO_2

$$CF_3OCO_2^\bullet \rightarrow CO_2 + CF_3O^\bullet \quad (5)$$

Within the temperature range studied in this work, k_5 should leave no chance of reaction −4 occurring. We can conclude that the rate limiting step in the mechanism must be reaction 4 to which all the parameters measured for $CF_3OC(O)OOC(O)F$ correspond.

When using N_2 as diluent, $CF_3OOC(O)F$ and CF_2O are formed; the appearance of the former could be easily explained through the reaction of $CF_3O^\bullet$ and the longer-lived $FCO_2^\bullet$

$$CF_3O^\bullet + FCO_2^\bullet \rightarrow CF_3OOC(O)F \quad (6)$$

whereas CF_2O comes from the unimolecular decomposition of $CF_3O^\bullet$

$$CF_3O^\bullet \rightarrow CF_2O + F^\bullet \quad (7)$$

When CO was used as bath gas, the products were the same as with N_2 plus $CF_3OC(O)F$ and an unidentified substance. Reactions 4−7 certainly occur in this system, but CO can also react with both $CF_3O^\bullet$ radicals to form $CF_3OC(O)^\bullet$—a reaction that has proved to be efficient and fast[11,22]—and with $F^\bullet$ atoms to form $FCO^\bullet$ in the reactions

$$CO + CF_3O^\bullet \rightarrow CF_3OC(O)^\bullet \quad (8)$$

$$CO + F^\bullet \rightarrow FC(O)^\bullet \quad (9)$$

$CF_3OC(O)F$ could be formed through the combination of $CF_3O^\bullet$ and $FC(O)^\bullet$, as is shown in reaction 10. The unknown substance could result from the combination of $CF_3OC(O)^\bullet$ and $FCO_x^\bullet$ ($x = 1$ or 2) radicals (reactions 11 and 12)

$$CF_3O^\bullet + FC(O)^\bullet \rightarrow CF_3OC(O)F \quad (10)$$

$$CF_3OC(O)^\bullet + FC(O)^\bullet \rightarrow CF_3OC(O)C(O)F \quad (11)$$

$$CF_3OC(O)^\bullet + FCO_2^\bullet \rightarrow CF_3OC(O)OC(O)F \quad (12)$$

Future work should be done either to confirm the above-proposed mechanism or to prove the existence of these new FCO molecules. The isolation and bulk manipulation of this kind of molecules could be of great help for atmospheric chemistry studies, since they could act as clean sources of $CF_3OCO_x^\bullet$ and $FCO_x^\bullet$ ($x = 0$, 1, or 2) radicals.

$CF_3OC(O)OOCF_3$. The first step in the pyrolysis mechanism produces $CF_3OCO_2^\bullet$ and $CF_3O^\bullet$ radicals

$$CF_3OC(O)OOCF_3 \rightarrow CF_3OCO_2^\bullet + CF_3O^\bullet \quad (13)$$

Occurrence of the back reaction (reaction −13) can be ruled out, once again because of the low stability of the $CF_3OCO_2^\bullet$ radicals at the temperatures studied and the fact that there was no difference between the decomposition rate constants obtained with the different diluents. The fate of $CF_3O^\bullet$ radicals in N_2 is either their decomposition (reaction 7) or recombination (reaction 14)

$$2CF_3O^\bullet \rightarrow CF_3OOCF_3 \quad (14)$$

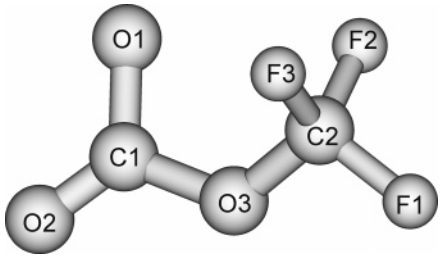

Figure 7. Calculated structure (B3LYP/6-31+G*) of the $CF_3OCO_2^\bullet$ radical.

TABLE 3: Ab Initio Geometrical Parameters of the $CF_3OCO_2^\bullet$ Radical

	B3LYP		MP2(FULL)	CBS-4M
	6-31G	6-311+G*	6-311+G*	
	Bond Lengths (Å)			
O(1)−C(1)	1.284	1.233	1.325	1.176
O(2)−C(1)	1.260	1.251	1.192	1.368
C(1)−O(3)	1.387	1.356	1.373	1.369
O(3)−C(2)	1.405	1.390	1.378	1.368
C(2)−F(1)	1.362	1.324	1.317	1.320
C(2)−F(2)	1.376	1.333	1.331	1.335
C(2)−F(3)	1.376	1.333	1.331	1.335
	Bond Angles (deg)			
O(1)−C(1)−O(2)	118.91	117.41	122.65	125.13
C(1)−O(3)−C(2)	121.98	120.49	121.28	126.32
O(3)−C(2)−F(1)	106.64	106.33	106.67	107.98
F(2)−C(2)−F(3)	108.50	108.94	108.24	108.05
O(1)−C(1)−O(3)−C(2)	−0.02	0.00	−0.75	−14.18
O(2)−C(1)−O(3)−C(2)	179.98	180.00	179.31	166.42
C(1)−O(3)−C(2)−F(1)	−179.98	−180.00	−179.93	−179.19

In CO as diluent, $CF_3OC(O)^\bullet$ radicals are formed through reaction 8, and their recombination gives the oxalate $(CF_3OC(O))_2$

$$2CF_3OC(O)^\bullet \rightarrow (CF_3OC(O))_2 \quad (15)$$

At the rather high temperatures used for decomposition, the reaction of $CF_3O^\bullet$ with CO also produces $CF_3^\bullet$ radicals[23]

$$CF_3O^\bullet + CO \rightarrow CF_3^\bullet + CO_2 \quad (16)$$

which react with $CF_3OC(O)^\bullet$ to yield the $CF_3OC(O)CF_3$ obtained

$$CF_3OC(O)^\bullet + CF_3^\bullet \rightarrow CF_3OC(O)CF_3 \quad (17)$$

Theoretical Calculations of the $CF_3OCO_2^\bullet$ Radical. Since it is difficult to obtain experimental data about spectroscopic and thermochemical properties for short-lived species, like the $CF_3OCO_2^\bullet$ radical, theoretical models based on electronic structure have become a proper tool for investigation and prediction of such properties. In the next sections, we provide geometrical parameters, vibrational frequencies, and heats of formation of this radical by using different ab initio methods.

Geometrical Parameters. At first glance, there are two different possibilities for the conformation of the acyloxy radical, both comprising the C_s symmetry group. The plane formed by the $-CO_2$ moiety could be parallel (A) or perpendicular (B) to the C−O−C−F chain. However, calculations starting with B geometry converged to A in all cases. The geometry obtained through the B3LYP/6-31+G* method is presented in Figure 7, where atom labeling is used to identify the different geometrical parameters.

Table 3 shows the structural parameters found with the different methods studied. In a general overview, small differ-

ences can be observed for B3LYP values with both basis sets. Significant differences in the dihedral angles are found with the MP2(FULL) and CBS-4 methods. These observations confirm that geometrical parameters have a strong dependence on the methods used. Since no experimental bond lengths and angles are available for the acyloxy radical, the calculated data are compared with the results of previous studies. Fortunately, the geometry of some compounds formed by F, C, and O has been precisely elucidated by the gas electron diffraction (GED) technique in conjunction with theoretical calculations. Molecules such as $(CF_3OC(O)O)_2$,[24] $CF_3OOC(O)F$,[25] $CF_3OC(O)F$, and $CF_3OC(O)OCF_3$[26] can be taken as model compounds to check the calculated geometrical parameters of $CF_3OCO_2^{\bullet}$.

The most interesting features of this radical are the bond lengths associated with the $-CO_2$ moiety (O(1)−C(1)−O(2)). The π character of the radical has recently been demonstrated,[15] and this indicates that due to a resonance effect both C−O distances should be equal. As can be seen from Table 3, with the B3LYP method, these distances are quite similar for both basis sets. Typical GED values for double bonded C═O atoms in fluorocarbooxygenated molecules are 1.177 Å ($CF_3OC(O)OOC(O)OCF_3$),[24] 1.188 Å ($CF_3OC(O)F$ and $CF_3OC(O)OCF_3$),[26] and 1.190 Å ($CF_3C(O)OOC(O)CF_3$).[27] Single bonded C−O values are 1.364 Å ($CF_3OC(O)F$), 1.377 Å ($CF_3OC(O)OCF_3$),[26] and 1.361 Å ($CF_3C(O)OOC(O)CF_3$).[27] Thus, the C−O bond lengths for the resonant $-CO_2$ moiety are expected to be somewhere between the above values. For the $FCO_2^{\bullet}$ radical with C_{2v} symmetry, at the QCISD/6-31G* level, an r(CO) distance of 1.245 Å was calculated and an experimental value of 1.288 Å was suggested.[19] Only theoretical values have been reported for the $CF_3CO_2^{\bullet}$ radical. At the UMP2/6-31G* level, two values were obtained:[28] $r(CO) = 1.209$ Å and $r(CO') = 1.337$ Å. Von Ahsen et al.[4] have recalculated the $CF_3CO_2^{\bullet}$ radical with the B3LYP/6-311(d,p) method, but unfortunately, no geometrical parameters have been reported.

As can be seen from Table 3, B3LYP values for $CF_3OCO_2^{\bullet}$ with both basis sets agree with what is expected for the length of a resonant bond, although the difference between both CO lengths, Δr(CO) (|O(1)−C(1)−O(2)−C(1)|), is smaller for the 6-311+G* ($\Delta r(CO) = 0.018$ Å) than for the 6-31G ($\Delta r(CO) = 0.024$ Å) basis set. The MP2 and CBS-4M values gave differences in the bond lengths that correspond to a σ radical with one oxygen double bonded and the other single bonded to C(1).

It is also important to notice that B3LYP differs from MP2 and CBS-4 in the value obtained for the O(1)−C(1)−O(2) bond angle. In the first case, 118.91 and 117.41° are predicted with 6-31G and 6-311+G*, respectively, in good agreement with the OCO angle for the $FCO_2^{\bullet}$ radical, for which 119 ± 1° was reported as the experimental value.[19] With the MP2(FULL)/6-311+G* and CBS-4 methods, 122.65 and 125.13° are obtained, respectively. These last two values correspond to an O═C−O angle where one oxygen is double bonded to the carbon atom. Some experimental values for the O═C−O angle are 127.4° ($CF_3OC(O)OOC(O)OCF_3$),[24] 128.5° ($CF_3OC(O)OCF_3$), 130.3° ($CF_3OC(O)F$),[26] and 129.6° ($CF_3OOC(O)F$).[25]

Bond lengths associated with O−C(sp^3) and O−C(sp^2) bonds present differences which are too small, for example, in $CF_3OC(O)F$, O−C(sp^3) = 1.379 Å and O−C(sp^2) = 1.349 Å, in $CF_3OC(O)OCF_3$, O−C(sp^3) = 1.389 Å and O−C(sp^2) = 1.365 Å, and in $CF_3OOC(O)F$, O−C(sp^3) = 1.393 Å and O−C(sp^2) = 1.376 Å. As can be observed, O−C(sp^2) bonds are shorter than O−C(sp^3) bonds. For $CF_3OCO_2^{\bullet}$, this tendency is well reproduced with the B3LYP and MP2(FULL)/6-311+G* methods, but the latter gives a difference which is too small; both bond lengths are almost equal when using the CBS-4M method. A qualitative explanation can be given for the difference in terms of a partial delocalization effect between the three oxygen atoms in the $O-CO_2$ moiety. Since the electron correlation and the basis set are very important factors affecting delocalization, the CBS-4 method (where geometries are calculated with a HF wave function) does not describe it properly.

C−F bond distances are well reproduced by all methods. Typical GED values are 1.322 Å ($CF_3OC(O)F$),[26] 1.315 Å ($CF_3OC(O)OCF_3$),[26] and 1.317 Å ($(CF_3OC(O)O)_2$).[24]

It can be concluded that, for the geometrical parameters of this radical, B3LYP methods give better results than the others. The resonance effect between the O(1)−C(1)−O(2) atoms, which was demonstrated experimentally by using isotopically marked compounds,[15] is reproduced only by B3LYP methods for which interatomic C(1)−O(1 or 2) bond lengths and the O(1)−C(1)−O(2) angle are similar and comparable with the same parameters in the $FCO_2^{\bullet}$ radical. The rest of the geometrical parameters agree quite well with what is expected for an "F−C−O" radical compared with experimental values of similar molecules.

Vibrational Frequencies. The vibrational frequencies for the $CF_3OCO_2^{\bullet}$ radical obtained at the B3LYP/6-311+G* level are presented in Table 4.

Assuming C_s symmetry for the $CF_3OCO_2^{\bullet}$ radical, all 18 fundamental modes should be IR-active according to the irreducible representation of the vibrations given in eq 18:

$$\Gamma_{vib} = 12A'(\text{IR,Ra p}) + 6A''(\text{IR, Ra dp}) \qquad (18)$$

Due to the similar masses and comparable bond strengths of all atoms, the modes in the radical are strongly mixed, except for the carbonyl stretching. In Table 4, an approximate description of each mode is given in terms of the dominant coordinate(s).

Table 4 also shows the fundamental modes of the related radicals $CF_3OC(O)^{\bullet}$,[4] $CF_3OC(O)O_2^{\bullet}$,[3] and $FCO_2^{\bullet}$.[19] Considering the CF_3O- fragment as a pseudo-halogen, the properties of the $-CO_2$ moiety should be similar in both $FCO_2^{\bullet}$ and $CF_3OCO_2^{\bullet}$. Indeed, the wavenumbers of ν_1 ($-CO_2$ stretching) are similar for these radicals and are red shifted (around 400 cm^{-1}) with respect to ν_1 (the C═O stretching) for $CF_3OC(O)^{\bullet}$ and $CF_3OC(O)O_2^{\bullet}$. This vibration is predicted to be at higher wavenumbers in $CF_3OCO_2^{\bullet}$ than in $FCO_2^{\bullet}$, since the force constant for the mode is affected by the group attached to the carbon atom. Fluorine should have a higher withdrawing effect than that of the CF_3O- group on the unpaired electron, lowering the force constant of the $-CO_2$ vibration.

In the region between 1300 and 850 cm^{-1}, six stretching modes are expected. The most intense bands at 1255, 1208, 1202, and 1128 cm^{-1} are assigned to ν_2, ν_{13}, ν_3, and ν_4 and described as C−F/C−O stretching, as in the case of other similar radicals with a CF_3O- fragment. The other two stretching modes, ν_5 and ν_6, correspond mainly to the C−O−C asymmetric and symmetric vibrations.

Heat of Formation of the $CF_3OCO_2^{\bullet}$ Radical. To obtain the heat of formation of this radical, two approaches were used. One is based on isodesmic reaction 19. Due to the fact that in this kind of reactions the reactants and products contain the same number of bonds of the same type, errors due to limitation in

TABLE 4: Ab Initio Calculated Frequencies (B3LYP/6-31+G*) and Approximate Assignment of IR Modes of the $CF_3OCO_2^•$ Radical and Related Compounds

$CF_3OC(O)$[a]					$CF_3OC(O)O_2$ ttt[b]					CF_3OCO_2			FCO_2[c]					assignment acc to C_s symmetry	
exptl		calcd			exptl		calcd			calcd			exptl		calcd				
ν (cm^{-1})	int[d]	ν (cm^{-1})	int	mod	ν (cm^{-1})	int	ν (cm^{-1})	int	mod	ν (cm^{-1})	int	mod	ν (cm^{-1})	int	ν (cm^{-1})	int	mod		description
1857	16	1927	36	A′	1895	62	1945	43	A′	1528	65	A′	1475	100	1494	100	a1	ν_1	ν C′O_2
1280	83	1282	84	A′	1295	100	1286	41	A′	1255	78	A′	960	42	983	19	a1	ν_2	ν_s CF_3
1203	100	1191	100	A′	1207	35	1206	15	A′	1202	45	A′	519	9	521	7.2	a1	ν_3	ν CF_3/C′O_2
997	52	1026	53	A′	1170	75	1178	37	A′	1128	100	A′	1098	47	1047	74	b1	ν_4	ν_s CF_3
902	11	903	8.6	A′	1087	59	1115	100	A′	1056	4.4	A′	474	9	491	4.2	b1	ν_5	ν_a C−O−C′
720	1.3	718	1.9	A′	936	24	935	20	A′	856	2.6	A′	735	9	731	16	b2	ν_6	ν_s C−O−C′
612	0.8	608	0.92	A′	895	1.9	892	0.41	A′	738	6	A′						ν_7	δ_{oop} O−C′O_2
457	0.5	472	0.56	A′	740	1.4	758	0.43	A′	724	1.5	A′						ν_8	δ CF_3/OC′O
418	2.9	415	0.56	A′	694	7.5	692	4.5	A′	622	8.6	A′						ν_9	δ_s CF_3
		191	0.40	A′			557	0.02	A′	539	0.78	A′						ν_{10}	δ_s CF_3
1236	45	1230	73	A″	401	1.4	397	0.34	A′	403	0.28	A′						ν_{11}	ρ C′O_2
612	0.8	612	0.46	A″			376	0.12	A′	372	0.00	A′						ν_{12}	ρ CF_3
		430	0.02	A″			308	0.16	A′	1208	73	A″						ν_{13}	ν_a CF_3
		187	0.9	A″			151	0.14	A′	604	0.15	A″						ν_{14}	δ_a CF_3
		86	0.00	A″	1254	81	1245	49	A″	423	0.09	A″						ν_{15}	ω CF_3
					717	10	723	3.6	A″	163	0.08	A″						ν_{16}	δ COC′
							607	0.09	A″	89	0.07	A″						ν_{17}	τ FCOC′
							428	0.05	A″	58	0.00	A″						ν_{18}	τ F_2C/CO_2
							138	0.00	A″									ν_{19}	
							82	0.06	A″									ν_{20}	
							62	0.00	A″									ν_{21}	

[a] According to ref 37. [b] According to ref 38. [c] According to ref 35. [d] Relative intensities.

the basis set and electron correlation energy nearly cancel.

$$CF_3OCO_2^• + 2CH_3OH \rightarrow CH_3OCH_3 + CO_2 + CF_3OH + OH^• \quad (19)$$

The other approach is based on atomization reaction 20. Viskolcz and Bérces[29] have studied the enthalpy of formation of selected carbonyl radicals, some of them halogenated. They have obtained very good results calculating the heats of formation according to an atomization reaction (version B in ref 29) that requires the experimental enthalpies of formation for the appropriate atoms at 298 K. The atomization reaction for $CF_3OCO_2^•$ is

$$CF_3OCO_2^• \rightarrow 2C + 3F + 3O \quad (20)$$

According to this reaction, the atomization enthalpy at 298 K is obtained from the computed total energies, including zero point energies, and the thermal corrections for each species. The enthalpy of formation of $CF_3OCO_2^•$ is calculated according to

$$\Delta_f H^\circ_{298}(CF_3OCO_2^•) = 3 \times \Delta_f H^\circ_{298}(O) + 3 \times \Delta_f H^\circ_{298}(F) + 2 \times \Delta_f H^\circ_{298}(C) - \Delta_r H^\circ_{298} \quad (21)$$

Viskolcz et al.[29] concluded that the enthalpies of formation of species with halogen containing R groups are best characterized by the CBS-4 method by comparison with other models based on complete basis set extrapolation, such as G2(MP2,-SVP). The CBS-4 model was assessed using the G2 neutral test set of 148 molecules[30] by Curtiss et al.[31] The calculated enthalpies of formation showed an absolute deviation of 3.06 kcal mol^{-1} with experiment. The average absolute deviation obtained from Table 1 of ref 31 using only the fluorinated species is 3.32 kcal mol^{-1}. In the present paper, the atomization and isodesmic reaction energies were evaluated at the CBS-4 level.

The reaction enthalpies computed at 298 K are $\Delta_r H^\circ = -20$ kcal mol^{-1} for reaction 19 and $\Delta_r H^\circ_{16} = 806$ kcal mol^{-1} for reaction 20. Using the following experimental heats of formation at 298 K (JPL library,[32] units in kilocalories per mole): O (59.62 ± 0.02), F (19.00 ± 0.07), C (171.5 ± 0.1), OH (8.9 ± 0.1), CF_3OH (−218 ± 2), CO_2 (−94.14 ± 0.02), CH_3OCH_3 (−44.0 ± 0.1), and CH_3OH (−48.1 ± 0.1), the heat of formation $\Delta_f H^\circ_{298}(CF_3OCO_2^•)$ is −231 ± 2 kcal mol^{-1} for isodesmic reaction 19 and −227 ± 2 kcal mol^{-1} for atomization reaction 20. The uncertainties are mainly due to the experimental values (CF_3OH in particular). The enthalpy of formation for the radical should be obtained as the average value $\Delta_f H^\circ_{298}(CF_3OCO_2^•) = -229 \pm 4$ kcal mol^{-1}. The predicted value and the values $\Delta_f H^\circ_{298}(CF_3O^•) = -149$ kcal mol^{-1} and $\Delta_f H^\circ_{298}(CO_2) = -94.14$ kcal mol^{-1} lead to a reaction enthalpy of −14 kcal mol^{-1} for reaction 22

$$CF_3OCO_2^• \rightarrow CF_3O^• + CO_2 \quad (22)$$

This decarboxylation enthalpy can be compared with that for reaction $FCO_2^• \rightarrow F^• + CO_2$. The enthalpy obtained, using $\Delta_f H^\circ_{298}(FCO_2^•) = -86$ kcal mol^{-1},[33] is 11 kcal mol^{-1}. The more exothermic reaction is precisely the decarboxylation of the CF_3-$OCO_2^•$ radical, whose lifetime decreases because of this propensity to form more stable species.

Evaluation of the Heats of Formation of $CF_3OC(O)OOC$-(O)F, $CF_3OC(O)OOCF_3$, and $CF_3OC(O)OOC(O)OCF_3$. The heats of formation of $CF_3OC(O)OOC(O)F$ and $CF_3OC(O)$-$OOCF_3$ were derived from the rate constants by performing second law calculations. Within this approach, the heat of formation is obtained from the Arrhenius activation energy, which provides the heat of reaction $\Delta_r H^\circ = RT^2(\partial \ln k_1/\partial T)$ for reactions 4 and 13.

For $CF_3OC(O)OOC(O)F$, $E_a = \Delta_{r,1} H^\circ = 29$ kcal mol^{-1} and $\Delta_f H^\circ_{298}$ are obtained from the expression

$$\Delta_f H^\circ_{298}(CF_3OC(O)OOC(O)F) = \Delta_f H^\circ_{298}(CF_3OCO_2^•) + \Delta_f H^\circ_{298}(FCO_2^•) - \Delta_r H^\circ$$

Using for $\Delta_f H^\circ_{298}(CF_3OCO_2^•)$ the value obtained in this work and for $\Delta_f H^\circ_{298}(FCO_2^•)$ −86 kcal mol^{-1}, the heat of formation

of $CF_3OC(O)OOC(O)F$ is $\Delta_f H^\circ_{298}(CF_3OC(O)OOC(O)F) = -286 \pm 6$ kcal mol^{-1}.

By a similar procedure, but using reaction 13, we obtained -341 ± 6 kcal mol^{-1} as the heat of formation of $CF_3OC(O)OOCF_3$. We also calculated the heat of formation for the symmetric peroxide $CF_3OC(O)OOC(O)OCF_3$, which upon dissociation gives two $CF_3OCO_2^\bullet$ radicals as -430 ± 6 kcal mol^{-1}.

A general overview of the bond energies for the three peroxides—$CF_3OC(O)OOC(O)OCF_3$, $CF_3OC(O)OOC(O)F$, and $CF_3OC(O)OOCF_3$ (29, 29, and 34 kcal mol^{-1}, respectively)—clearly shows that they increase when the peroxydic bond is directly attached to a group having a large electron withdrawing capacity. In addition to that, the bond energies show how the carbonyl group blocks the withdrawing effect of either the F− or CF_3O− groups (whose influence should be almost the same due to the pseudo-halogen character of the $CF_3O^\bullet$ radical). The three compounds could be used in the laboratory as good thermal sources of $CF_3O^\bullet$ radicals at room or higher temperatures, while the possibility of obtaining the $CF_3OCO_2^\bullet$ radical is conditioned by the use of appropriate light and temperature low enough to induce the rupture and low temperatures that prevent the decarboxylation of the radical, as reported.[15] The availability of the heats of formation for the $CF_3OCO_2^\bullet$ radical and for these peroxides will probably help to further complete databases for atmospheric purposes.

Experimental Section

All volatile materials were manipulated in a glass vacuum line equipped with two capacitance pressure gauges (Bell and Howell and MKS Baratron 220) and three U-traps connected via glass valves with PTFE stopcocks (Young, London). The vacuum line was connected to a photoreactor, a thermal reactor, and a double-walled IR gas cell (optical path length 20 cm, Si windows 0.5 mm thick) placed in the sample compartment of a Fourier transform infrared (FTIR) spectrometer (Bruker IFS28). This arrangement made it possible to follow either the course of the synthesis, the purification processes, or the thermal decay of substances.

As the syntheses of $CF_3OC(O)OOC(O)F$[9] and $CF_3OC(O)OOCF_3$[5,7] have been reported before, only a brief description will be given here. Both were carried out in a 12 L round-bottom glass flask, with a central double-walled, water-jacketted quartz tube inside which a 40 W low pressure Hg lamp (Heraeus Hanau, Germany) was placed. The flask was connected to the vacuum line by means of PTFE stopcocks and flexible stainless steel bellows. The experiments were usually performed at temperatures close to −20 °C. $CF_3OC(O)OOC(O)F$ was obtained from the simultaneous photolysis in the gas phase of perfluoroacetic anhydride (5 mbar) and oxalyl fluoride (10 mbar) in the presence of CO (100 mbar) and O_2 (700 mbar). $CF_3OC(O)OOCF_3$ was obtained as a byproduct of the synthesis of $CF_3OC(O)OOC(O)OCF_3$ from the photolysis of perfluoroacetic anhydride (10 mbar) diluted in CO (10 mbar) and O_2 (700 mbar).

Due to their different thermal stabilities, each peroxide had to be studied under different temperature conditions. The thermal decomposition of $CF_3OC(O)OOC(O)F$ was studied using the double-walled IR cell in the sample compartment of the spectrometer. The outer jacket of the cell was connected to a thermostat, from which hot salty water flowed at temperatures ranging between 62 and 98 °C with an uncertainty of ±0.1 °C. Once the cell reached the intended temperature, 0.5−2 mbar of $CF_3OC(O)OOC(O)F$ was admitted and the pressure was immediately increased to either 1000 mbar with N_2 or 500 mbar with CO. After the reaction was started, a series of in situ timely spaced IR spectra were obtained. The data processing of the kinetic measurements was done using the absorption bands at 969 and 1874 cm^{-1}. The first was integrated over the range 980−954 cm^{-1}, and for the second, only the height of the band was considered. The IR spectra of the products were subtracted in all cases because of their interference with the absorption bands used for the analysis.

The thermal decomposition of $CF_3OC(O)OOCF_3$ was studied using a 2 L glass round-bottom flask thoroughly cleaned and immersed in a temperature-controlled bath of glycerin. The temperatures ranged between 130 and 165 °C with an uncertainty of ±0.5 °C. The reactor was loaded with different mixtures of $CF_3OC(O)OOCF_3$ diluted with either N_2 or CO in a ratio of 1:50 and with total pressures of up to 1000 mbar. The decomposition was started at a specified temperature by immersing the reactor in the bath, leaving the reaction to take place for a certain time and stopping it by sudden immersion of the reactor in an ice−water bath. A measured amount of the reaction mixture (the same for each experiment) was then allowed to expand into the IR cell to record one spectrum. The height of the absorption band at 1885 cm^{-1} was used to measure the decay without any subtraction because in this case the products did not interfere.

Most of the products obtained (CO_2, CF_3OOCF_3, $(CF_3OC(O))_2$, CF_2O, etc.) were identified from reference spectra of pure samples.

Perfluoroacetic anhydride (PCR, 98%), N_2 (AGA, 99.999%), O_2 (AGA, 99.9%), and CO (Praxair, 99%) were obtained from commercial samples and used without further purification.

Computational Details. Geometrical parameters and the heat of formation of the $CF_3OCO_2^\bullet$ radical were obtained by ab initio calculations. Three approaches were used to compare how some properties are described with different methods. Some calculations were done with the B3LYP method,[34−36] since a lot of computational studies exist where the density functional theory was successfully applied to molecules with C, O, and F.[8,27,37−41] Wave function methods based on basis set extrapolation have been successfully applied to obtain the thermochemical properties of simple hydrogenated and halogenated carbonyl radicals,[29] and therefore, some calculations were done with the CBS-4 method.[42] Finally, we also employed the widely used MP2(FULL)[43−45] method. The radical geometries were optimized using standard convergence criteria without symmetry restrictions. Frequencies were evaluated to check that the calculated geometry corresponded to a minimum in the potential energy surface and to evaluate the zero point energy. The 6-31G and 6-311+G* basis sets were used with the B3LYP method. All calculations were done with the Gaussian 98 program suite.[46]

Acknowledgment. We gratefully acknowledge financial support from Fundación Antorchas and CONICET, Argentina. M.A.B.P. wishes to thank CONICET for his postdoctoral fellowship. P.G. wants to thank PROALAR project for covering his travel expenses to Argentina. The authors thank Unidad de Matemática y Física of the Facultad de Ciencias Químicas for computer-cluster time. Language assistance from Karina Plasencia is gratefully acknowledged.

References and Notes

(1) Wallington, T. J.; Nielsen, O. J. *Handb. Environ. Chem.* **2002**, *3*, 85.

(2) Argüello, G. A.; Willner, H. *J. Phys. Chem. A* **2001**, *105*, 3466.

(3) von Ahsen, S.; Willner, H.; Francisco, J. S. *Chem.—Eur. J.* **2002**, *8*, 4675.

(4) von Ahsen, S.; Hufen, J.; Willner, H.; Francisco, J. S. *Chem.—Eur. J.* **2002**, *8*, 1189.
(5) Hohorst, F. A.; DesMarteau, D. D.; Anderson, L. R.; Gould, D. E.; Fox, W. B. *J. Am. Chem. Soc.* **1973**, *95*, 3866.
(6) Arvía, A. J.; Aymonino, P. J.; Schumacher, H. J. *An. Asoc. Quím. Argent.* **1962**, *50*, 135.
(7) Malanca, F. E.; Argüello, G. A.; Willner, H. *Inorg. Chem.* **2000**, *39*, 1195.
(8) Argüello, G. A.; von Ahsen, S.; Willner, H.; Burgos Paci, M. A.; García, P. *Chem.—Eur. J.* **2003**, *9*, 5135.
(9) Burgos Paci, M. A.; García, P.; Malanca, F. E.; Argüello, G. A.; Willner, H. *Inorg. Chem.* **2003**, *42*, 2131.
(10) Pernice, H.; Berkey, M.; Henkel, G.; Willner, H.; Argüello, G. A.; McKee, M. L.; Webb, T. R. *Angew. Chem.* **2004**, *116*, 2903.
(11) Malanca, F. E.; Burgos Paci, M. A.; Argüello, G. A. *J. Photochem. Photobiol., A* **2002**, *150*, 1.
(12) Kennedy, R. C.; Levy, J. B. *J. Phys. Chem.* **1972**, *76*, 3480.
(13) Czarnowski, J.; Schumacher, H. J. *Int. J. Chem. Kinet.* **1981**, *13*, 639.
(14) Burgos Paci, M. A.; Argüello, G. A.; García, P.; Willner, H. *Int. J. Chem. Kinet.* **2003**, *35*, 15.
(15) Burgos Paci, M. A.; Argüello, G. A. *Chem.—Eur. J.* **2004**, *10*, 1838.
(16) Rembaum, A.; Szwarc, M. *J. Am. Chem. Soc.* **1954**, *76*, 5.
(17) Czarnowski, J.; Schumacher, H. J. *Int. J. Chem. Kinet.* **1981**, *13*, 639.
(18) Cox, R. A.; Roffey, M. J. *Environ. Sci. Technol.* **1977**, *11* (9), 900.
(19) Argüello, G. A.; Grothe, H.; Kronberg, M.; Willner, H.; Mack, H.-G. *J. Phys. Chem.* **1995**, *99*, 17525.
(20) Wallington, T. J.; Hurley, M. D.; Matti Maricq, M. *Chem. Phys. Lett.* **1993**, *205*, 63.
(21) Matti Maricq, M.; Szente, J. J.; Khitrov, G. A.; Francisco, J. S. *J. Phys. Chem.* **1996**, *100*, 4514.
(22) Malanca, F. E.; Argüello, G. A.; Staricco, E. H.; Wayne, R. P. *J. Photochem. Photobiol., A* **1998**, *117*, 163.
(23) Czarnowski, J.; Schumacher, H. *Z. Phys. Chem.* **1974**, *92*, 329.
(24) Hnyk, D.; Machácek, J.; Argüello, G. A.; Willner, H.; Oberhammer, H. *J. Phys. Chem. A* **2003**, *107*, 847.
(25) Trautner, F.; Gholivand, K.; García, P.; Willner, H.; Erben, M. F.; Della Védoba, C.; Oberhammer, H. *Inorg. Chem.* **2003**, *42*, 3079.
(26) Hermann, A.; Trautner, F.; Gholivand, K.; vonAhsen, S.; Varetti, E. L.; DellaVedova, C. O.; Willner, H.; Oberhammer, H. *Inorg. Chem.* **2001**, *40*, 3979.
(27) Kopitzky, R.; Willner, H.; Hermann, A.; Oberhammer, H. *Inorg. Chem.* **2001**, *40*, 2693.
(28) Francisco, J. S. *Chem. Phys. Lett.* **1992**, *191*, 7.
(29) Viskolcz, B.; Bérces, T. *Phys. Chem. Chem. Phys.* **2000**, *2*, 5430.
(30) Curtiss, L. A.; Raghavachari, K.; Redfern, P. C.; Pople, J. A. *J. Chem. Phys.* **1997**, *106*, 1063.
(31) Curtiss, L. A.; Raghavachari, K.; Redfern, P. C.; Stefanov, B. B. *J. Chem. Phys.* **1998**, *108*, 692.
(32) Sander, S. P.; Friedl, R. R.; Golden, D. M.; Kurylo, M. J.; Huie, R. E.; Orkin, V. L.; Moortgat, G. K.; Ravishankara, A. R.; Kolb, C. E.; Molina, M. J.; Finlayson-Pitts, B. J. *Chemical kinetics and Photochemical Data for Use in Stratospheric Modeling. Evaluation 14, JPL Publ. 02-25* 2003.
(33) Dibble, T. S.; Francisco, J. S. *J. Phys. Chem.* **1994**, *98*, 11694.
(34) Lee, C.; Yang, W.; Parr, R. G. *Phys. Rev. B* **1988**, *41*, 785.
(35) Becke, A. D. *J. Chem. Phys.* **1993**, *98*, 5648.
(36) Becke, A. D. *J Chem. Phys.* **1993**, *98*, 1372.
(37) Ventura, O. N.; Kieninger, M. *Chem. Phys. Lett.* **1995**, *254*, 488.
(38) McKee, M. L.; Webb, T. R. *J. Phys. Chem.* **1996**, *100*, 11292.
(39) Pernice, H.; Willner, H.; Bierbrauer, K. L.; Burgos Paci, M. A.; Argüello, G. A. *Angew. Chem., Int. Ed. Engl.* **2002**, *41*, 3832.
(40) Badenes, M. P.; Castellano, E.; Cobos, C. J.; Croce, A. E.; Tucceri, M. E. *Chem. Phys. Lett.* **1999**, *303*, 482.
(41) Badenes, M. P.; Castellano, E.; Cobos, C. J.; Croce, A. E.; Tucceri, M. E. *Chem. Phys.* **2000**, *253*, 205.
(42) Ochterski, J. W.; Petersson, G. A.; Montgomery, J. A., Jr. *J. Chem. Phys.* **1996**, *104*, 2598.
(43) Head-Gordon, M.; Pople, J. A.; Frisch, M. J. *Chem. Phys. Lett.* **1988**, *153*, 503.
(44) Frisch, M. J.; Head-Gordon, M.; Pople, J. A. *Chem. Phys. Lett.* **1990**, *166*, 275.
(45) Frisch, M. J.; Head-Gordon, M.; Pople, J. A. *Chem. Phys. Lett.* **1990**, *166*, 281.
(46) Frisch, M. J.; Trucks, G. W.; Schlegel, H. B.; Scuseria, G. E.; Robb, M. A.; Cheeseman, J. R.; Zakrzewski, V. G.; Montgomery, J. A., Jr.; Stratmann, R. E.; Burant, J. C.; Dapprich, S.; Millam, J. M.; Daniels, A. D.; Kudin, K. N.; Strain, M. C.; Farkas, O.; Tomasi, J.; Barone, V.; Cossi, M.; Cammi, R.; Mennucci, B.; Pomelli, C.; Adamo, C.; Clifford, S.; Ochterski, J.; Petersson, G. A.; Ayala, P. Y.; Cui, Q.; Morokuma, K.; Malick, D. K.; Rabuck, A. D.; Raghavachari, K.; Foresman, J. B.; Cioslowski, J.; Ortiz, J. V.; Baboul, A. G.; Stefanov, B. B.; Liu, G.; Liashenko, A.; Piskorz, P.; Komaromi, I.; Gomperts, R.; Martin, R. L.; Fox, D. J.; Keith, T.; Al-Laham, M. A.; Peng, C. Y.; Nanayakkara, A.; Gonzalez, C.; Challacombe, M.; Gill, P. M. W.; Johnson, B.; Chen, W.; Wong, M. W.; Andres, J. L.; Gonzalez, C.; Head-Gordon, M.; Replogle, E. S.; Pople, J. A. *Gaussian 98*, revision A.7; Gaussian Inc.: Pittsburgh, PA, 1998.
(47) Rembaum, A.; Szwarc, M. *J. Am. Chem. Soc.* **1954**, *76*, 5975.
(48) Rembaum, A.; Szwarc, M. *J. Chem. Phys.* **1955**, *23*, 909.